Biochemistry and Biophysics Reports 5 (2016) 63–69

Contents lists available at ScienceDirect

Biochemistry and Biophysics Reports

journal homepage: www.elsevier.com/locate/bbrep

Splicing of human chloride channel 1

Takumi Nakamura [1], Natsumi Ohsawa-Yoshida [1], Yimeng Zhao, Michinori Koebis, Kosuke Oana, Hiroaki Mitsuhashi, Shoichi Ishiura *

Department of Life Science, Graduate School of Arts and Sciences, The University of Tokyo, 3-8-1 Komaba, Meguro-ku, Tokyo 153-8902, Japan

ARTICLE INFO

Article history:
Received 19 August 2015
Received in revised form
28 October 2015
Accepted 9 November 2015
Available online 11 November 2015

Keywords:
Myotonic dystrophy
MBNL1
Splicing
Human chloride channel 1 gene

ABSTRACT

Expression of *chloride channel 1* (*CLCN1*/*ClC-1*) in skeletal muscle is driven by alternative splicing, a process regulated in part by RNA-binding protein families MBNL and CELF. Aberrant splicing of *CLCN1* produces many mRNAs, which were translated into inactive proteins, resulting in myotonia in myotonic dystrophy (DM), a genetic disorder caused by the expansion of a CTG or CCTG repeat. This increase in abnormal splicing variants containing exons 6B, 7A or the insertion of a TAG stop codon just before exon 7 leads to a decrease in expression of the normal splice pattern. The majority of studies examining splicing in *CLCN1* have been performed using mouse *Clcn1*, as have investigations into the activation and suppression of normal splicing variant expression by *MBNL1-3* and *CELF3–6*, respectively. In contrast, examinations of human *CLCN1* have been less common due to the greater complexity of splicing patterns. Here, we constructed a minigene containing *CLCN1* exons 5–7 and established a novel assay system to quantify the expression of the normal splicing variant of *CLCN1* using real-time RT-PCR. Antisense oligonucleotides could promote normal *CLCN1* alternative splicing but the effective sequence was different from that of *Clcn1*. This result differs from previous reports using *Clcn1*, highlighting the effect of differences in splicing patterns between mice and humans.

1. Introduction

Myotonic dystrophy (*dystrophia myotonica*, DM) is an autosomal dominant disorder and the most common form of inherited muscular dystrophy in adults [1]. DM is characterised by a wide range of symptoms, including myotonia, progressive muscle loss, cataracts, cardiac conduction defects, insulin resistance and cognitive impairments [2]. Two forms of DM, DM1 and DM2, have been described to date. In DM1, disease symptoms result from an aberrant expansion of the CTG trinucleotide repeat in the 3′ untranslated region (UTR) in myotonic dystrophy protein kinase (*DMPK*) on chromosome 19 [3–5]. In DM2, disease is caused by an expansion of a CCTG tetranucleotide repeat in intron 1 of the CCHC-type zinc finger, nucleic acid binding protein (*CNBP*) gene on chromosome 3 [6]. Among patients with DM, several lines of evidence have suggested a relationship between transcribed RNA CUG or CCUG repeats and disease symptoms. First, the number of CUG repeats correlates with the severity of symptoms [5]. Second, in cells derived from patients with DM, expanded CUG and CCUG repeats accumulate in the nucleus [6–8]. Third, HSA^{LR} transgenic mice expressing an expanded CUG repeat inserted in the human skeletal muscle actin (*HSA*) gene manifest myotonia and abnormal muscle histology [9].

In addition to sequence repeats, abnormalities in RNA metabolism have also been found in patients with DM. Aberrant splicing has been reported in multiple genes, including chloride channel 1 (*CLCN1*), insulin receptor (*INSR*), bridging integrator 1 (*BIN1*), myomesin 1 (*MYOM1*) and actin-binding LIM protein 1 (*ABLIM1*), among others [10–14], leading to a variety of symptoms in these patients. This aberrant splicing is thought to be driven by two families of splicing factors, muscleblind-like (*MBNL*) and CUG binding protein/ELAV-like family (CELF). MBNL proteins MBNL1–3 bind CHG/CHHG (H: A, C and U) sequences of RNA and co-localise with mRNAs containing CUG expanded repeats [15]. This process leads to a decrease in the intracellular concentrations of functionally available MBNL proteins. Alternatively, CELF proteins, especially CELF1 and CELF2, are activated by CUG repeats, although the pathways regulating this process have not been fully elucidated [16]. This imbalance of MBNL and CELF in turn leads to abnormal splicing of downstream genes, further exacerbating DM symptoms.

Here, we examine the effects of MBNL1-3 and CELF1-6 on DM. *CLCN1* is thought to be responsible for myotonia, the most characteristic symptom in DM1 [17]. Many studies have been performed using mouse *Clcn1*. In these models, a frameshift occurs following

* Corresponding author.
E-mail address: cishiura@mail.ecc.u-tokyo.ac.jp (S. Ishiura).
[1] These authors have equally contributed to this work.

http://dx.doi.org/10.1016/j.bbrep.2015.11.006

the insertion of exon 7A (79 bp) between exon 6 and 7 in *Clcn1*; these immature mRNA transcripts are then degraded by the nonsense-mediated mRNA decay (NMD) machinery, resulting in lower steady state levels of CLCN1 protein. Correction of the abnormal splicing patterns in HSA^{LR} transgenic mice has been shown to rescue this phenotype, leading to recovery from myotonia [18]. Moreover, in *Clcn1*, MBNL1–3 decrease the insertion of exon 7A, whereas CELF3–6 increase it [19]. However, chloride channelopathy in DM1 has been reported to be due to downregulation of CLCN1 transcription [20]. So, the mechanism of myotonia in DM1 is controversial.

Far less is known regarding the function of human *CLCN1*, as mouse and human *CLCN1* exhibit distinctly different splicing patterns. *CLCN1* encodes for two additional exons, 6B (55 bp) not present in the mouse orthologue and 7A (79 bp) between exons 6 and 7; insertion of either or both of these exons into *Clcn1* results in a frameshift mutation. Alternative splicing of these exons has been shown to produce numerous variants in the skeletal muscle of patients with DM, including variants such as 5–6B–7A–7–8, 5–6–6B–7A–7–8 and 5–8 [17]. Beyond these two additional exons, another splicing pattern characterised by a three base pair (TAG triplet) extension of exon 7 has also been detected [10]. This inserted TAG sequence is thought to act as a stop codon, resulting in the production of the immature mRNA.

To better understand the mechanism of splicing in *CLCN1*, we began by constructing a minigene spanning exons 5–7 of *CLCN1*, resulting in the synthetic *CLCN1* (5–7) minigene. We also established a new assay using real-time reverse transcription (RT)-PCR, which can distinguish between splicing variants based upon the presence of the TAG-inserted pattern. We found significant differences between the human and mouse orthologue, which may have important implications for the study of DM.

2. Materials and methods

2.1. Cell culture, transfection and RNA extraction

HEK293 cells were grown in Dulbecco's modified Eagle's medium (DMEM) containing 10% foetal bovine serum (FBS) and subcultured at 90–100% confluence. HEK293 cells were plated at 6.0×10^5 cells on 6-well plates 24 h before transfection. For RT-PCR analyses, the *CLCN1* (5–7) minigene (1.0 μg) was transfected with 3.0 μL FuGENE 6 (Promega). In the cellular splicing assay, minigenes (0.2 μg) and splicing factor constructs (0.8 μg) were transfected with 3.0 μL FuGENE 6. For antisense analysis, HEK293 cells were cultured in 12-well plates and transfected with minigenes (0.1 μg) and AONs (antisense oligonucleotides: phosphorothioate 2′ *O*-methyl RNA oligonucleotides (Coralville, IA) listed in Supplementary Table ST1, 50 pmol) using 4.0 μL Lipofectamine 2000 at 50–60% confluence and incubated for 48 h; total RNA was extracted using a GenElute Mammalian Total RNA Miniprep Kit with DNase treatment (Sigma-Aldrich), as described previously [13,14,21].

2.2. RT-PCR and sequence analysis

For cDNA synthesis, 1.0 μg of total RNA was reverse-transcribed with a PrimeScript 1st Strand cDNA synthesis Kit (TaKaRa Bio) in a total volume of 10 μL using oligo(dT) primers. cDNA samples were then diluted fivefold prior to use. PCR was performed using Ex Taq DNA polymerase (TaKaRa Bio) according to the manufacturer's protocol. For sequence analysis of the *CLCN1* (5–7) minigene, PCR was carried out using the following primer set: forward (5′-CATGGTCCTGCTGGAGTTCGTG-3′) and reverse (5′-CTCCAAGTGGTGTCCCAAAACAAC-3′). PCR conditions were as follows: an initial denaturation step at 96 °C for 2 min, 30 cycles at 96 °C for 30 s, 62 °C for 30 s and 72 °C for 30 s, and a final extension step of 72 °C for 5 min. PCR products were then separated via 8% polyacrylamide gel electrophoresis and soaked in ethidium bromide solution (1 μg/ml); then the relevant bands were extracted from the gel. The spliced gel was shaken in solution buffer (0.5 M ammonium acetate and 1 mM EDTA in sterilised water) for 48 h, after which the products were washed in isopropyl alcohol followed by ethanol precipitation. Precipitates were then dissolved in a volume of 5 μL sterilised water. The purified DNA fragment was inserted into a pGEM-TEasy vector (Promega) using a Rapid DNA Ligation Kit (Roche) and sequenced to confirm proper insertion.

2.3. Real-time PCR

Expression of the normal splicing pattern variant of *CLCN1* was quantified using a relative standard curve method following amplification on a StepOnePlus Real-Time PCR System (Life Technologies). Reactions were performed using the Power SYBR Green PCR Master Mix (Life Technologies). PCR reaction was performed in a total volume of 10 μL using cDNA samples (1 μL). PCR conditions were as follows: an initial denaturation step at 96 °C for 20 s, followed by 40–55 cycles at 96 °C for 30 s and 67 °C for 30 s, and a final melt curve step at 96 °C for 30 s, 67 °C for 30 s and 96 °C for 30 s. Expression of the normal splicing pattern was compared against the expression of GFP in the *CLCN1* (5–7) minigene relative to the mock control. Each threshold cycle value (Ct-value) was calculated as an average of three replicates, with undetermined values treated as 0. Another mock sample (pcDNA3.1) was used as the control baseline for calculating relative quantification (RQ) value. The normal splicing pattern was amplified using the *CLCN1* (5–6–7) primer set: forward (5′-GTTCTGCGGGGTATATGAaCA-3′) and reverse (5′-CTCCAAGTGGTGTCCCAAAACAAC-3′); GFP was amplified using the following primers: forward (5′-AAGTTCAGCGTGTCCGG-3′) and reverse (5′-TGTCGCCCTCGAACTTC-3′). Each primer set was adjusted to a final concentration of 500 nM.

2.4. Standard curve

To draw the standard curve, initial templates were diluted in sterile water and supplemented with 0.2 pg/μL salmon sperm single strand DNA (D1626, Sigma), followed by a series of four ninefold dilutions. The pGEM-TEasy vector (Promega) containing the normal splicing pattern insert was used as the control template at a starting concentration of 1 ng/μL. GFP controls were amplified from mock control cDNA. Variance between replicates due to high annealing and extension temperatures was limited by using standard curves with an $R^2 > 0.95$.

2.5. Protein extraction

Transfected cells were harvested in sonication buffer (0.1% Triton X-100, 0.1% protease inhibitor mix in phosphate-buffered saline, PBS) and disrupted 10 times by sonication using Sonifier 450 disruptor (Branson) with an output of 3 and a duty cycle of 10%. After sonication, protein concentrations were quantified using a DC Protein Assay (Bio-Rad) according to the manufacturer's instructions. Briefly, each sample was diluted to 2 μg/μL with PBS and diluted twofold in 2 × sample buffer to a final concentration of 1 μg/μL. Samples were stored at −80 °C.

2.6. Western blotting

Samples were resolved by SDS-PAGE and transferred to PVDF membranes (Immobilon-P, Millipore). The membranes were then blocked with 5% skim milk in PBS with 0.05% Tween 20 (PBST) for 1 h at room temperature and then incubated overnight at 4 °C with primary antibodies, anti-myc (1:5000, R950-25; Invitrogen)

and anti-actin (1:600, Spring Bioscience) in 5% skim milk. After washing, the membranes were incubated for 1 h in horseradish peroxidase (HRP)-conjugated secondary antibodies (Cell Signaling Technologies) at room temperature. The immunoreactive bands were visualised by enhanced chemiluminescence (ECL) and scanned using an LAS-3000 image analyser (FujiFilm).

2.7. Constructs

The *CLCN1* (5–7) minigene was constructed using the *CLCN1* minigene [19], which spans exons 6–7 of *CLCN1*. The genomic fragment covering exon 5 and intron 5 was amplified by nested PCR using PrimeSTAR GXL DNA Polymerase (TaKaRa Bio) from human genomic DNA (Promega). The first fragment containing exons 5–6 was amplified using the following primer set: forward (5′-AGAACTTGCCACCAGACTCG-3′) and reverse (5′-TGGACTAG-CAGGGAGAGCAT-3′). The second fragment was amplified using the first fragment as template with the following primers: forward (5′-AAAGATCTGGAATCCCCGAAATGAA-3′) and reverse (5′-TGGAC-TAGCAGGGAGAGCAT-3′). The second fragment was then inserted into the BglII–XapI site of the *CLCN1* minigene and sequenced to confirm proper recombination. Splicing factors MBNL1, MBNL2, MBNL3, CELF1, CELF2, CELF3, CELF4, CELF5 and CELF6 were cloned as described previously into pSec-DK, a mammalian expression vector with a myc-tag and 6× His-tag modified from pSecTagA (Invitrogen) by deleting the Igκ chain leader sequence [19].

2.8. Mutagenesis

The first fragment of the *CLCN1* (A > T) minigene and the second fragment of the *CLCN1*(ΔTAG) minigene were amplified with PrimeSTAR GXL DNA Polymerase (TaKaRa Bio) using the *CLCN1*(5–7) minigene as a template. The following primer sets were used for PCR amplification: first fragment, forward (5′-CTCTGTCTGTCTCTCCCCTtGTAGCAGCCATACTACTACTCTG-3′) and reverse (5′-CAGAGTAGTAGTATGGCTGCTACaAGGGG-AGAGACAGACAGAG-3′) and second fragment, forward (5′-CCTGTTTCTCTGTCTGTCTCTCCCC_TAGCAGCCATACTACTACTCTG-3′) and reverse (5′-CAGAGTAGTAGTATGGCTGCTA_GGGGAGA-GACAGACAGAGAAACAGG-3′). PCR products were then treated with DpnI and inserted into the HindIII–SalI site of the *CLCN1* (5–7) minigene. Each minigene was sequenced before use to confirm proper insertion.

3. Results

3.1. Splicing pattern of the CLCN1 (5–7) minigene

This study was performed using the *CLCN1* (5–7) minigene, which consisted of exons 5–7 of *CLCN1* inserted into a pEGFP-C1 expression vector (Fig. 1A). This vector was then transfected into HEK293 cells and analysed by RT-PCR to compare the splicing patterns of the human construct to that of the mouse orthologue (Fig. 1B). Several splicing patterns were observed, including exons 5–6–6B–7A–7, 5–6B–7A–7 and 5–6–7 [17]. These patterns are in stark contrast to that of *Clcn1*, which contains only exons 5–6–7 and 5–6–7A–7 (Fig. 1). As frameshifts are known to occur in all constructs expressing exons 6B or 7A, these splicing variants are likely to result in the production of inactive proteins or mRNAs, which would be degraded via nonsense-mediated mRNA decay (NMD). The normal spliced band containing exons 5–6–7 (286 bp) and an abnormally spliced one containing exons 5–7A–7 (287 bp) were indistinguishable by electrophoresis, limiting our ability to quantify production of the normal splice variant.

3.2. Reappearance of the TAG-inserted pattern in the CLCN1 (5–7) minigene

During the analysis of the *CLCN1* (5–7) minigene splicing, we detected an additional splicing variants containing a TAG sequence just before exon 7 (Fig. 2A). We refer to this splicing pattern as the "TAG-inserted pattern". This splicing pattern was found in exons 5–7A–7, 5–7 and 5–6–7, suggesting that a TAG sequence can exist in each of the bands shown in Fig. 1B. Because the TAG sequence encodes for a stop codon, these splicing variants also produce the mRNAs which are translated into inactive proteins. The frequency of the TAG-inserted pattern has previously been investigated across all splicing variants of *CLCN1* [10]. Here, we performed RT-PCR followed by sequencing of the 5–6–7 splice band from human skeletal muscle biopsies to determine the ratio of the TAG-inserted pattern relative to that of the 5–6–7 splicing pattern (Fig. 2B). The observed ratio was found to be highly variable between individuals, with no significant difference in the percentage of the TAG inserted pattern between DM and controls.

To determine the mechanism underlying TAG insertion, we examined the sequence immediately upstream of exon 7, revealing two tandem TAG sequences (Fig. 2C). We hypothesised that the

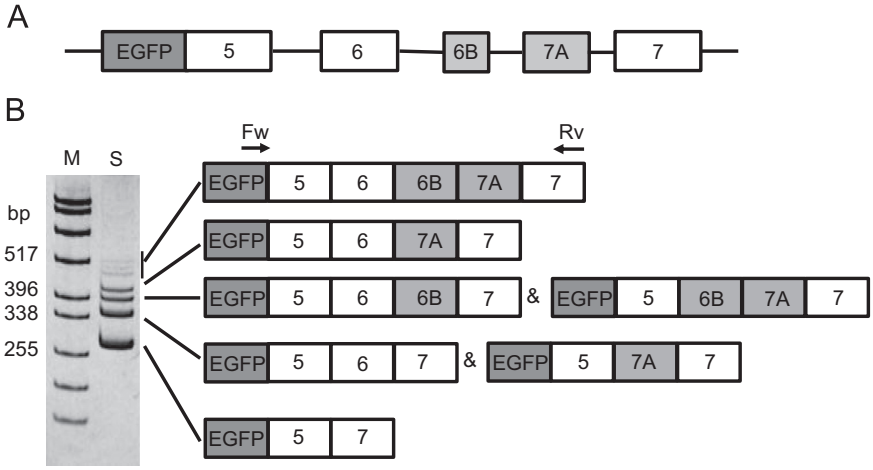

Fig. 1. Splicing patterns of the *CLCN1* (5–7) minigene. (A) Structure of the *CLCN1* (5–7) minigene. Exons 5–7 of *CLCN1* were inserted downstream of EGFP. Frameshifts occur in splicing variants having each or both of exons 6B and 7A, which may result in the production of immature proteins. (B) The *CLCN1* (5–7) minigene was transfected into HEK293 cells, and the resulting splicing variants were analysed by RT-PCR. Various other splicing patterns were also detected; however, the splicing variant containing only exons 5–7 was not detected in human muscle. M, marker; S. splicing products, bp, base pair. Since we used a forward primer which is complementary to GFP sequence, appeared bands are higher than the theoretical ones.

A

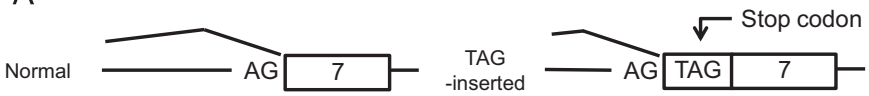

B

Sample	Normal	TAG-inserted	TAG (%)
Non-DM1	12	3	20
Non-DM2	9	6	40
Non-DM3	12	3	20
Non-DM4	15	0	0
Non-DM5	11	4	27
DM1	10	5	33
DM2	8	7	47
DM3	11	4	27
DM4	13	2	13
DM5	9	6	40

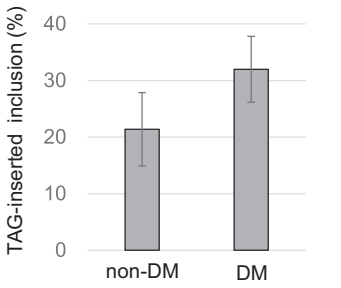

***P=0.2518
(Student's t-test; mean ± SD; n = 5)

C

D

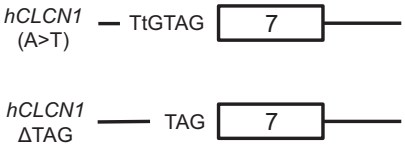

E

	Normal	TAG-inserted	TAG-inserted inclusion (%)
hCLCN1	5	15	75
hCLCN1(A>T)	20	0	0
hCLCN1(ΔTAG)	20	0	0

Fig. 2. Analysis of the TAG-inserted pattern. (A) The structure of the TAG-inserted pattern. In this pattern, a TAG sequence that encodes for a stop codon is inserted immediately upstream of exon 7. (B) The percentage of the TAG-inserted pattern in normal-sized splicing variants in human skeletal muscle biopsies (Non-DM1-5: 8mo(M), 2y(M), 31y(F), 34y(M), 42y(M), respectively ; DM1-5: 8mo(M), 2y(M), 11y(M), 36y(M), 41y(M), respectively). We performed RT-PCR and sequenced the band corresponding to the normal splicing pattern 15 times for each individual. Interindividual variances in the percentage of TAG-inserted pattern transcripts were evident, but these differences were not significantly different between DM and control groups. (C) Sequences adjacent to exon 7. Two tandemly repeated TAG sequences were detected just before exon 7. (D) Analysis of the acceptor site in TAG-inserted pattern transcripts. Two mutant *CLCN1* minigenes were constructed: *CLCN1* (A > T), in which the TAG sequence was mutated to TTG, and *CLCN1*ΔTAG, in which the TAG sequence was deleted. (E) Analysis of the percentage of the TAG-inserted pattern inclusion in each construct. The TAG-inserted pattern was completely absent in each of the two mutant constructs.

upstream TAG sequence serves as the acceptor site for mRNA splicing. To confirm this hypothesis, we generated two constructs: one in which the upstream TAG sequence was mutated to TTG, *CLCN1* (A > T), and the other in which the upstream TAG sequence was deleted, *CLCN1*ΔTAG (Fig. 2D). These constructs were then transfected into HEK293 cells, and the resulting transcripts were analysed by RT-PCR and sequenced. The TAG-inserted pattern was shown to be completely lost in each construct (Fig. 2E), indicating that the upstream TAG sequence, particularly the 'AG' residues, serves as the new acceptor site to produce the TAG-inserted pattern.

3.3. Establishment of a new assay system to quantify the normal splicing pattern variant

Based upon the various splicing patterns observed in the first round of analyses, we developed a new assay to quantify the normal splicing pattern variant by real-time RT-PCR using a primer set specific for those sequences. In this assay, the forward primer annealed to the junction of exons 6 and 7, and the reverse primer annealed to exon 7. Complementarity between the two bases on the 5′ end of exon 7 was used to distinguish the 5–6–7 splicing variant from that of the TAG-inserted pattern (Fig. 3A, left). However, as this forward primer is also complementary to a portion of the TAG-inserted pattern (Fig. 3A, right), this primer set was able to amplify both the 5–6–7 and the TAG-inserted patterns under standard PCR conditions. Next, we designed the forward primer to have one mismatch in the four bases complementary to the TAG-inserted pattern, so that the complementarity between the primer and the TAG-inserted pattern is suppressed (Fig. 3B). This primer set was referred to as *CLCN1* (5–6–7).

Finally, we optimised our PCR conditions using the *CLCN1* (5–6–7) primer set. Generally, real-time PCR is performed in two steps containing a single denaturation followed by an annealing and extension step. Plasmid vectors containing the 5–6–7 and the TAG-inserted pattern sequences were used as the template and analysed by gradient PCR. Specific amplification of the 5–6–7 splicing pattern was observed at temperatures > 67.1 °C (Fig. 3C);

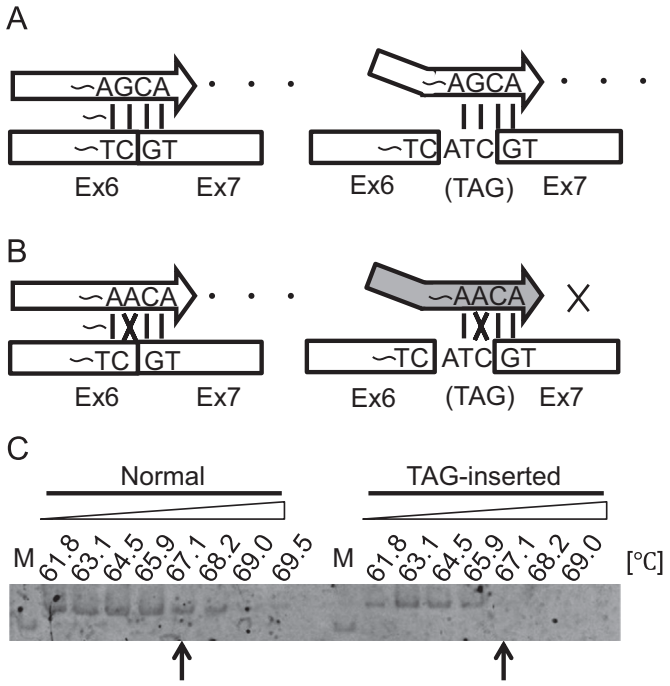

Fig. 3. The establishment of the assay system. (A) The original primer set. Theoretically, the forward primer should anneal to the junction of exons 6 and 7, resulting in specific amplification of the normal splicing pattern; however, this forward primer is complementary to a portion of the TAG-inserted pattern, resulting in amplification of this region under standard PCR conditions. (B) A schematic diagram of the *CLCN1* (5–7) forward primer. The original primer was modified to include one mismatch in the last four bases complementary to the TAG-inserted pattern, allowing for specific amplification of the normal splicing pattern. (C) Optimisation of the annealing and extension steps using the *CLCN1* (5–7) primer set. Gradient PCR was performed in two steps using a denaturation step of 96 °C for 30 s, followed by a 30 s annealing and extension step using the pGEM-TEasy plasmid vector containing the normal or TAG-inserted pattern as template. The following temperatures for annealing and extension were used: 61.8 °C, 63.1 °C, 64.5 °C, 65.9 °C, 67.1 °C, 68.2 °C, 69.0 °C and 69.5 °C. Of these conditions, 67.1 °C was chosen as the optimal temperature for specific amplification of the normal splicing pattern.

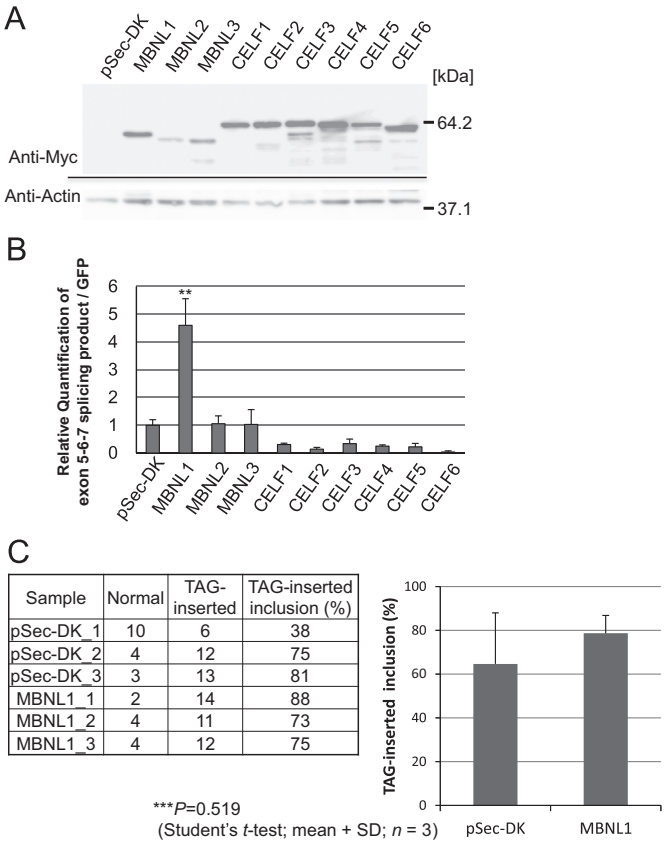

Sample	Normal	TAG-inserted	TAG-inserted inclusion (%)
pSec-DK_1	10	6	38
pSec-DK_2	4	12	75
pSec-DK_3	3	13	81
MBNL1_1	2	14	88
MBNL1_2	4	11	73
MBNL1_3	4	12	75

Fig. 4. Results of the cellular splicing assay in HEK293 cells. (A) The expression of each splicing factor was verified by Western blot. Splicing factor constructs (0.8 μg) and the *CLCN1* (5–7) minigene (0.2 μg) were co-transfected into HEK293 cells. Anti-Myc antibody was used to detect each splicing factor containing a Myc tag; anti-Actin was used as an internal control. (B) Expression of the *CLCN1* normal splicing pattern by real-time RT-PCR, relative to the expression of GFP in the *CLCN1* (5–7) minigene. *MBNL1* induced a 4.5-fold increase in the expression of the normal splicing pattern relative to controls; these effects were not seen with either *MBNL2* or *MBNL3*. In contrast, CELF proteins tended to downregulate the expression of the normal splicing pattern ($n=3$). Bars indicate the mean and SEM; statistical significance was evaluated using Dunnett's multiple comparison test ($^{**}p < 0.05$). (C) The percentage of the TAG-inserted pattern in HEK293 cells co-transfected with *CLCN1* (5-7) minigene and MBNL1/pSec-DK (each $n=3$). We performed RT-PCR and sequenced the band corresponding to the normal splicing pattern 15–16 times for each sample as the experiment of Fig. 2B. But, the percentage of TAG-inserted inclusion did not change upon MBNL1 overexpression.

we therefore set the annealing and extension temperature for all subsequent PCRs at 67 °C when using the *CLCN1* (5–6–7) primer set. Suitability of these conditions was validated by real-time PCR (data not shown).

3.4. Quantification of the normal splicing pattern of CLCN1

To investigate the effects of splicing factors MBNL1-3 and CELF1-6, we performed a cellular splicing assay using the quantification method described above. Expression of each splicing factor was confirmed by Western blot (Fig. 4A). Expression of MBNL1 significantly increased the expression of 5–6–7 splicing pattern transcripts 4.5-fold relative to controls; these effects were not seen with either MBNL2 or MBNL3. These results are in stark contrast to that of a previous report performed using *Clcn1* [19], highlighting the difference between human and mouse transcripts. Moreover, CELF families tended to downregulate the expression of the 5–6–7 splicing pattern (Fig. 4B).

To confirm whether MBNL1 regulates TAG-insertion splicing, we performed normal RT-PCR and sequenced the band corresponding to the normal splicing pattern 15–16 times for each cell sample co-transfected with minigene and MBNL1/pSec-DK (Fig. 4C). The ratio of TAG-inserted inclusion condition did not change at all upon MBNL1 overexpression. MBNL1 increased not only normal isoform but also TAG-inserted isoform. Therefore, we conclude that MBNL1 does not regulate the TAG-insertion splicing, but promotes exon 6B and/or exon 7A skipping.

3.5. AONs induced exclusion of CLCN1 exons 6B and 7A

Next, we investigated whether AONs could induce 5–6–7 splicing of *CLCN1* using the quantification method described above (Fig. 5). Exon 7A (+63−8) AON significantly induced a 4-fold increase in the expression of the 5–6–7 splicing pattern relative to the control. Exon 7A (−10+15) AON also tends to increase the expression of 5–6–7 splicing product. But other AONs did not enhance 5–6–7 splicing. In the previous study, AON of exon 7a (+1+25) on *Clcn1* efficiently excluded exon 7a *in vitro* and *in vivo* [23]. However, AON of exon 7a (+1+25) did not induce 5–6–7 splicing of *CLCN1*.

4. Discussion

Here, we investigated human specific splicing of *CLCN1*, the gene responsible for myotonia in DM, using an *CLCN1* (5–7)

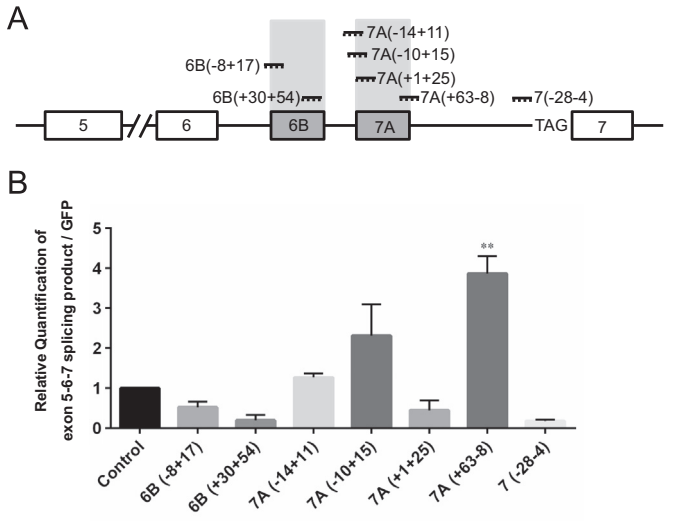

Fig. 5. AON-mediated exclusion of CLCN1 exons 6B and 7A in HEK293 cells. (A) Locations of the target sites of AONs (thick black lines) along the *CLCN1* pre-mRNA. (B) Results of the cellular splicing assay by AON in HEK293 cells. Expression of the *CLCN1* 5–6–7 splicing product by real-time RT-PCR, relative to the expression of all transcipts in the *CLCN1* (5–7) minigene, was shown. Exon 7A (+63−8) AON was the most successful AON for inducing 5–6–7 splicing of *CLCN1* minigene in HEK293 cells ($n=3$). Exon 7A (+63−8) AON induced a 4-fold increase in the expression of the 5–6–7 splicing pattern relative to controls. Also, Exon 7A (−10+15) AON tends to induce 5–6–7 splicing, whereas exon7A (+1+25) does not. Bars indicate the mean and SEM; statistical significance was evaluated using Dunnett's multiple comparison test ($^{**}p < 0.01$).

minigene expression construct. Expression of this minigene revealed various splicing patterns, including the TAG-inserted pattern, which encodes for a stop codon and is readily detected in human skeletal muscle biopsies. To distinguish between these various transcripts, we developed an RT-PCR assay specific for the 5–6–7 splicing pattern, regardless of the presence of other variants. This assay was then used to quantify cellular splicing. MBNL1 was shown to activate the expression of the 5–6–7 splicing pattern, with no effects seen for either MBNL2 or MBNL3. This result marks an important difference from that of our previous reports using mouse *Clcn1* [19]. In contrast to MBNL1, overexpression of each CELF isoform decreased the expression of the 5–6–7 splicing pattern.

The TAG-inserted pattern is likely the cause of myotonia, as it produces a stop codon just before exon 7 and can suppress the expression of the 5–6–7 splicing pattern. Although we detected the acceptor site responsible for this insertion, the overall function of the TAG-inserted pattern remains unclear. In terms of its role in DM, no significant differences were observed in the percentage of 5–6–7 and TAG-inserted patterns between DM and controls. However, as sequencing was performed only 15 times per individual, comparisons between these two groups may not be fully reliable. We therefore needed to establish an assay that could be used to specifically quantify the TAG-inserted pattern, as well as investigate the TAG-inserted pattern in more detail. In this study, we identified two tandemly repeated TAG sequences immediately upstream of exon 7, one of which served as the splice acceptor site for this exon. These two TAG sequences are conserved across a range of species, including chimpanzees, dogs and mice, and have been used in a variety of experiments investigating *Clcn1* [10]. Hence, a more accurate assay method like the one described here may be necessary for future examinations of *Clcn1*.

The assay system described here is able to directly quantify the production of 5–6–7 splicing pattern transcripts, an important distinction as the expression of this protein is directly related to the onset of myotonia. However, this assay was unable to quantify other splicing variants. We will therefore need to establish additional assays such as direct RNA sequencing as a means of quantifying the percentage of each splicing variant to better understand the effects of splicing in *CLCN1*. Furthermore, this assay relied on real-time PCR performed at relatively high annealing and extension temperatures to achieve transcript-specific amplification of the normal splicing pattern. As a result, variance in Ct-values between triplicates was detected. Further improvements will be necessary to fully quantify the various splicing products produced by this gene.

Using this new assay, we were able to detect differences in terms of *CLCN1* regulation between MBNL1 and MBNL2-3. All three MBNL proteins bind CHG/CHHG sequences of RNA and have the same amount of zinc finger domains, which are critical for recognising a common consensus sequence in pre-mRNA and mRNA targets [22]. Splicing efficacy therefore depends on differences in the target genes themselves, as opposed to any specific MBNL protein. In fact, our previous reports showed that the effects of each isoform differed based upon its target genes [13,14]. On the other hand, the expression levels of MBNL2 and MBNL3 are weaker than that of MBNL1 (Fig. 4A), which may have mediated the lower overall effects seen with these homologues. However, in our previous study using *Clcn1*, we observed a similar tendency in terms of protein expression; however, in this model, both MBNL2 and MBNL3 did enhance the expression of the 5–6–7 splicing pattern [19]. Moreover, the effects of MBNL are regulated by a variety of other factors, such as the secondary structure of mRNAs [22].

AON successfully alleviated the myotonic phenotype in DM model mice [18,23]. To screen for an optimal AON sequence, we used 25-mer phosphorothioate 2′ *O*-methyl RNA molecules that covered the exon 6B or exon 7A. Unexpectedly, AON 7A (+63−8) which covers the boundary of intron 7A and exon 7A enhanced the expression of 5–6–7 splicing product. Some AONs designed on exon 7A excluded not only exon 7A but also exon 6B (Fig. 5). Therefore we thought that the exclusion of exons 6B and 7A might be related. AON of exon 7A (+1+25) which was the most successful AON in mice did not enhance 5–6–7 splicing in human. We therefore hypothesise that the differences seen between mice and humans are the result of sequence differences between the human and mouse orthologues of *CLCN1*, as sequence similarity in exons 5–7 is only 75% according to BLAST analysis.

In this study, we described differences in splicing patterns of *Clcn1* and *CLCN1*. These observations are important, as they suggest that results obtained using *Clcn1* do not necessarily apply to *CLCN1*. Subsequent experiments should therefore focus on *CLCN1*, as opposed to the mouse *Clcn1* in investigations on *CLCN1* for DM medical treatments.

Acknowledgements

We thank Dr. Yoshihiro Kino for providing the *CLCN1* minigene. We also thank Dr. Satoshi Suo, Ms. Kurara Takagane, Ms. Shoin Tei, Mr. Takashi Nagashima, Mr. Ryo Yonezawa and Mr. Hiroshige Ishii for valuable discussions. This work was supported in part by an Intramural Research Grant (MHLW;26-8) for Neurological and Psychiatric Disorders of NCNP, a research grant for Comprehensive Research on Disability Health and Welfare from the Ministry of Health, Labour and Welfare (MHLW; H26-Sinkeikinn-ippan-004) and a Grant-in-Aid from the MHLW of Japan (to S.I.).

Appendix A. Supplementary material

Supplementary data associated with this article can be found in the online version at http://dx.doi.org/10.1016/j.bbrep.2015.11.006.

References

[1] G. Meola, R. Cardani, Myotonic dystrophies: an update on clinical aspects, genetic, pathology, and molecular pathomechanisms, Biochem. Biophys. Acta 1852 (2015) 594–606.
[2] P.S. Harper, Myotonic Dystrophy, third ed., W.B. Saunders, London, 2001.
[3] J.D. Brook, et al., Molecular basis of myotonic dystrophy: expansion of a trinucleotide (CTG) repeat at the 3′ end of a transcript encoding a protein kinase family member, Cell 68 (1992) 799–808.
[4] Y.H. Fu, D.L. Friedman, S. Richard, J.A. Pearlman, R.A. Gibbs, A. Pizzuti, T. Ashizawa, M.B. Perryman, G. Scarlato, R.G. Fenwick, et al., Decreased expression of myotonin-protein kinase messenger RNA and protein in adult form of myotonic dystrophy, Science 260 (1993) 235–238.
[5] M. Mahadevan, C. Tshilfidis, L. Sabourin, G. Shutler, C. Amemiya, G. Jansen, C. Neville, M. Narang, J. Barcelo, K. O'Hoy, et al., Myotonic dystrophy mutation: an unstable CTG repeat in the 3′ untranslated region of the gene, Science 255 (1992) 1253–1255.
[6] C.L. Liquori, K. Ricker, M.L. Moseley, J.F. Jacobsen, W. Kress, S.L. Naylor, J. Day, L. P.W. Ranum, Myotonic dystrophy type 2 caused by a CCTG expansion in intron 1 of ZNF9, Science 293 (2001) 864–867.
[7] K.L. Taneja, M. McCurrach, M. Schalling, D. Housman, R.H. Singer, Foci of trinucleotide repeat transcripts in nuclei of myotonic dystrophy cells and tissues, J. Cell Biol. 128 (1995) 995–1002.
[8] B.M. Davis, M. McCurranch, K.L. Taneja, R.H. Singer, D.E. Housman, Expansion of a CUG trinucleotide repeat in the 3′ untranslated region of myotonic dystrophy protein kinase transcripts results in nuclear retention of transcripts, Proc. Natl. Acad. Sci. USA 94 (1997) 7388–7393.
[9] A. Mankodi, E. Logigian, L. Callahan, C. McClain, R. White, D. Henderson, M. Krym, C.A. Thornton, Myotonic dystrophy in transgenic mice expressing an expanded CUG repeat, Science 289 (2000) 1769–1773.
[10] A. Mankodi, M.P. Takahashi, H. Jiang, C.L. Beck, W.J. Bowers, R.T. Moxley, S. C. Cannon, C.A. Thornton, Expanded CUG repeats trigger aberrant splicing of ClC-1 chloride channel 1 pre-mRNA and hyperexcitability of skeletal muscle in myotonic dystrophy, Mol. Cell 10 (2002) 35–44.
[11] R.S. Savkur, A.V. Philips, T.A. Cooper, Aberrant regulation of insulin receptor alternative splicing is associated with insulin resistance in myotonic dystrophy, Nat. Genet. 29 (2001) 40–47.
[12] C. Fugier, A.F. Klein, C. Hammer, S. Vassilopoulos, Y. Ivarsson, A. Toussaint, V. Tosch, A. Vignaud, A. Ferry, N. Messaddeq, Y. Kokunai, R. Tsuburaya, P. de la Grange, D. Dembele, V. Francois, G. Precigout, C. Boulade-Ladame, M. C. Hummel, A. Lopez de Munain, N. Sergeant, A. Laquerriere, C. Thibault, F. Derychere, D. Auboeuf, L. Garcia, P. Zimmerann, B. Udd, B. Schoser, M. P. Takahashi, I. Nishino, G. Bassez, J. Laporte, D. Furling, N. Charlet-Berguerand, Misregulated alternative splicing of BIN1 is associated with T tubule alterations and muscle weakness in myotonic dystrophy, Nat. Med. 17 (2011) 720–725.
[13] M. Koebis, N. Ohsawa, Y. Kino, N. Sasagawa, I. Nishino, S. Ishiura, Alternative splicing of myomesin 1 gene is aberrantly regulated in myotonic dystrophy type 1, Genes Cells 16 (2010) 961–972.
[14] N. Ohsawa, M. Koebis, H. Mitsuhashi, I. Nishino, S. Ishiura, ABLIM1 splicing is abnormal in skeletal muscle of patients with DM1 and regulated by MBNL, CELF, and PTBP1, Genes Cells 20 (2015) 121–134.
[15] M. Fardaei, M.T. Rogers, H.M. Thorpe, K. Larkin, M.G. Hamshere, P.S. Harper, J. D. Brook, Three proteins, MBNL, MBLL and MBXL, co-localize *in vivo* with nuclear foci of expanded-repeat transcripts in DM1 and DM2 cells, Hum. Mol. Genet. 11 (2002) 805–814.
[16] R. Roberts, N.A. Timchenko, J.W. Miller, S. Reddy, C.T. Caskey, M.S. Swanson, L. T. Timchenko, Altered phosphorylation and intracellular distribution of a (CUG)n triplet repeat RNA-binding protein in patients with myotonic dystrophy and in myotonin protein kinase knockout mice, Proc. Natl. Acad. Sci. USA 94 (1997) 13221–13226.
[17] B.N. Charlet, R.S. Savkur, G. Singh, A.V. Philips, E.A. Grice, T.A. Cooper, Loss of the muscle-specific chloride channel in type 1 myotonic dystrophy due to misregulated alternative splicing, Mol. Cell 10 (2002) 45–53.
[18] T.M. Wheeler, J.D. Lueck, M.S. Swanson, R.T. Dirksen, C.A. Thornton, Correction of ClC-1 splicing eliminates chloride channelopathy and myotonia in mouse models of myotonic dystrophy, J. Clin. Investig. 117 (2007) 3952–3957.
[19] Y. Kino, C. Washizu, Y. Oma, H. Onishi, Y. Nezu, N. Sasagawa, N. Nukina, S. Ishiura, MBNL and CELF proteins regulate alternative splicing of the skeletal muscle chloride channel CLCN1, Nucleic Acids Res. 37 (2009) 6477–6490.
[20] A. Ehralidze, Y. Wang, V. Petkova, K. Ehralidze, R.P. Junghaus, RNA leaching of transcription factors disrupts transcription in myotonic dystrophy, Science 303 (2004) 383–387.
[21] N. Ohsawa, M. Koebis, S. Suo, I. Nishino, S. Ishiura, Alternative splicing of PDLIM3/ALP, for alpha-actin-associated LIM protein 3, is aberrant in persons with myotonic dystrophy, Biochem. Biophys. Res. Commun. 409 (2011) 64–69.
[22] P. Konieczny, E. Stepniak-Konieczna, K. Sobczak, MBNL proteins and their target RNAs, interaction and splicing regulation, Nucleic Acids Res. 42 (2014) 10873–10887.
[23] M. Koebis, T. Kiyatake, H. Yamaura, K. Nagano, M. Higashihara, M. Sonoo, Y. Hayashi, Y. Negishi, Y. Endo-Takahashi, D. Yanagihara, R. Matsuda, M. P. Takahashi, I. Nishino, S. Ishiura, Ultrasound-enhanced delivery of morpholino with Bubble liposomes ameliorates the myotonia of myotonic dystrophy model mice, Sci. Rep. 3 (2013) 2242.